Pyrrolobenzoxazepinone Derivatives as Non-Nucleoside HIV-1 RT Inhibitors: Further Structure−Activity Relationship Studies and Identification of More Potent Broad-Spectrum HIV-1 RT Inhibitors with Antiviral Activity

Giuseppe Campiani,*,§ Elena Morelli,‖ Monica Fabbrini,‖ Vito Nacci,‖ Giovanni Greco,⊥ Ettore Novellino,⊥ Anna Ramunno,⊥ Giovanni Maga,‡ Silvio Spadari,‡ Giuseppe Caliendo,⊥ Alberto Bergamini,† Emanuela Faggioli,† Ilaria Uccella,† Francesca Bolacchi,† Stefano Marini,⊗ Massimiliano Coletta,⊗ Angelo Nacca,▽ and Silvio Caccia▽

Dipartimento di Scienze Farmaceutiche, Facolta' di Farmacia, Universita' degli Studi di Salerno, via Ponte don Melillo, 84084 Fisciano (SA), Italy, Dipartimento Farmaco Chimico Tecnologico, Facolta' di Farmacia, Universita' degli Studi di Siena, via Aldo Moro, 53100 Siena, Italy, Dipartimento di Chimica Farmaceutica e Tossicologica, Universita' di Napoli "Federico II", via D. Montesano 49, 80131 Napoli, Italy, Dipartimento di Sanita' Pubblica e Biologia Cellulare (DSP&BC) and Dipartimento di Medicina Sperimentale e Scienze Biochimiche (DMSSB), Universita' degli Studi di Roma "Tor Vergata", via Tor Vergata 135, 00133 Roma, Italy, Istituto di Genetica Biochimica ed Evoluzionistica (IGBE) - CNR, via Abbiategrasso 207, 27100 Pavia, Italy, and Istituto di Ricerche Farmacologiche "Mario Negri", via Eritrea 62, 20157 Milano, Italy

Received March 30, 1999

Pyrrolobenzoxazepinone (PBO) derivatives represent a new class of human immunodeficiency virus type 1 (HIV-1) non-nucleoside reverse transcriptase (RT) inhibitors (NNRTs) whose prototype is (±)-6-ethyl-6-phenylpyrrolo[2,1-*d*][1,5]benzoxazepin-7(6*H*)-one (**6**). Docking studies based on the three-dimensional structure of RT prompted the synthesis and biological evaluation of novel derivatives and analogues of **6** featuring a meta-substituted phenyl or a 2-thienyl ring at C-6 and a pyridine system in place of the fused-benzene ring to yield pyrrolopyridooxazepinones (PPOs). Compared with the lead **6** and nevirapine, several of the synthesized compounds (PBOs **13a**−**d** and PPOs **13i**−**k**) displayed higher inhibitory activity against wild-type RT and clinically relevant mutant RTs containing the single amino acid substitutions L100I, K103N, V106A, Y181I, and Y188L. The most potent inhibitors were further evaluated for in vitro antiviral activity on lymphocytes and monocyte-macrophages, for cytotoxicity on a panel of cell lines, and for potential synergistic antiviral activity with AZT. Pharmacokinetic studies performed on **13b**, **13c**, and **13i** showed that these compounds achieve high concentrations in the brain. The results of the biological and pharmacokinetic experiments suggest a potential clinical utility of analogues such as **13b**−**d**, **13i**, and **13j**, in combination with nucleoside RT inhibitors, against strains of HIV-1 bearing those mutations that confer resistance to known NNRTI.

Introduction

Reverse transcriptase (RT) is a key multifunctional enzyme in the life cycle of the type-1 human immunodeficiency virus (HIV-1). The enzyme shows both RNA- and DNA-dependent polymerase activities and is responsible for conversion of the single-stranded RNA retroviral genome into the double-stranded proviral DNA, which is successively integrated into the host cell chromosome.[1] Although several targets for therapeutic intervention have been identified in the life cycle of HIV-1, the lack of RT activity in the eukaryotic cells has made RT one of the most attractive targets for the development of anti-HIV-1 agents.[2−5] Its inhibition is considered one of the most practicable approaches to prevent the spread of infection. The RT inhibitors known to date can be divided into two main classes: nucleoside inhibitors (NRTIs) that interact competitively with the catalytic site of the RT and the non-nucleoside inhibitors (NNRTIs) that inhibit the enzyme by an allosteric interaction with a site adjacent to the NRTI binding site. A competitive inhibitor (NRTI) currently employed in the treatment of acquired immune deficiency syndrome (AIDS) is AZT (**1**), but its therapeutic usefulness is limited by poor brain penetration, emergence of viral resistance, toxicity, and low specificity.[6−8] NNRTIs have been found to bypass some of the disadvantages inherent to nucleoside inhibitors, but despite high specificity, their therapeutic effectiveness is limited by the onset of skin rashes and the rapid development of resistance. Representative compounds of the NNRTI class are nevirapine (**2**),[9] TIBO compounds (**3**),[10] thioureas such as trovirdine (**4**),[11] and pyridone derivatives (**5**).[12] Although these compounds are structurally unrelated, they interact with the allosteric site of RT by a similar three-dimensional arrangement.[13] We have recently described a new class of NNRTIs based on a pyrrolobenzoxazepinone (PBO) structure (**6**)[14] (Chart 1). The most potent compound was (±)-6-ethyl-6-phenylpyrrolo[2,1-*d*][1,5]benzoxazepin-7(6*H*)-one (**6**) which had significant antiviral efficacy but

* To whom correspondence should be addressed. Tel: +39-089-962809. Fax: +39-089-962828. E-mail: campiani@unisa.it.
§ Universita' degli Studi di Salerno.
‖ Universita' degli Studi di Siena.
⊥ Universita' degli Studi di Napoli "Federico II".
‡ IGBE - CNR.
† DSP&BC, Universita' degli Studi di Roma "Tor Vergata".
⊗ DMSSB, Universita' degli Studi di Roma "Tor Vergata".
▽ Istituto di Ricerche Farmacologiche "Mario Negri".

10.1021/jm990150o CCC: $18.00 © 1999 American Chemical Society
Published on Web 10/05/1999

Chart 1

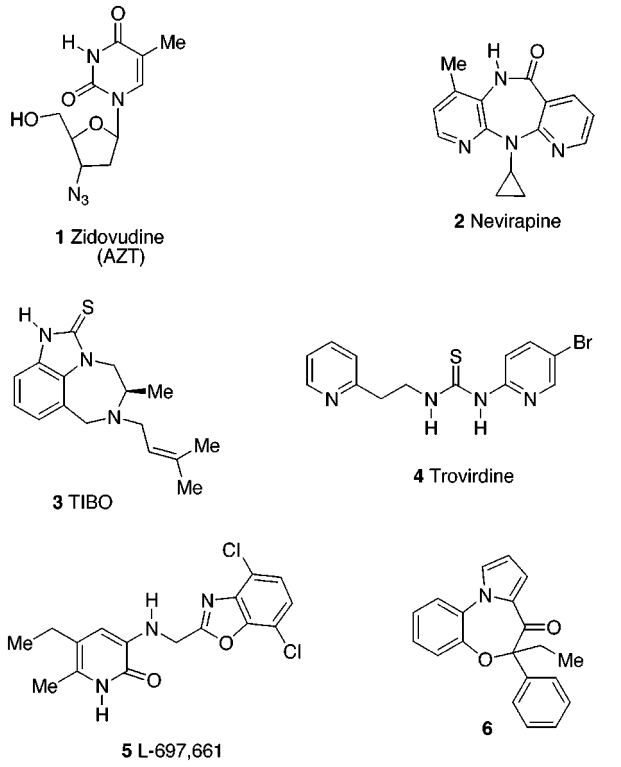

Chart 2. Planned Modifications to Our Lead and the Newly Designed Antiviral Agents

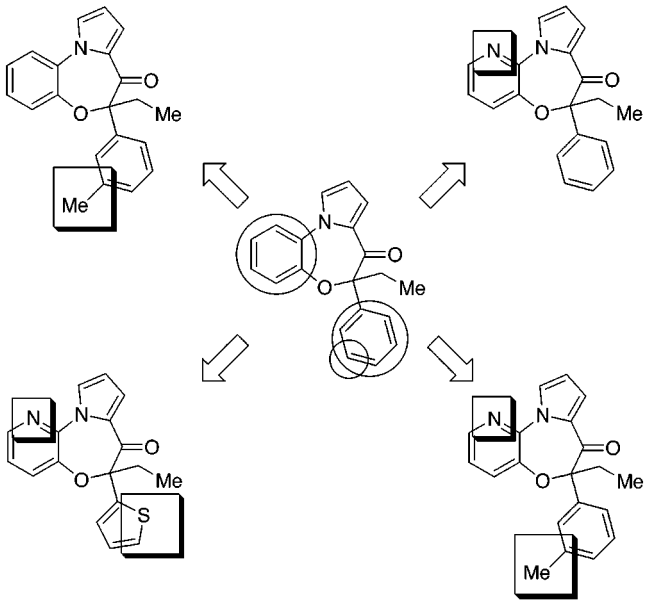

limited spectrum of activity. To improve the pharmacological properties of this lead, and to further explore the potential of PBOs as anti-HIV agents, additional compounds in this series were designed by docking studies based on the structure of wild-type RT (Chart 2). The compounds were then tested as inhibitors of RTwt and mutant RTs as well as for inhibition of HIV-1 replication in T4 lymphocytes and monocyte-macrophages. This strategy led to the identification of anti-HIV-1 agents with greater inhibitory potency and broader spectrum compared with **6** or nevirapine. We also report synergistic antiretroviral activity with AZT

Scheme 1

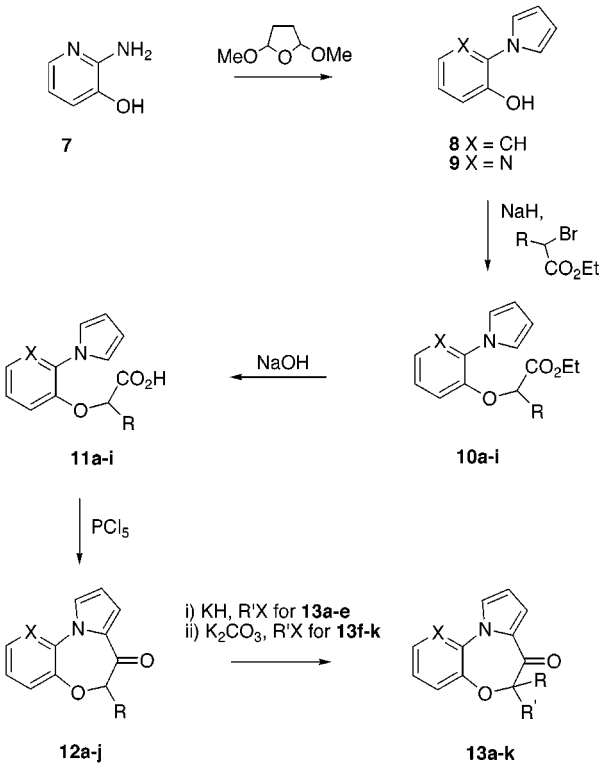

	X	R	R'
a	CH	*m*-FPh	Et
b	CH	*m*-OMePh	Et
c	CH	*m*-tolyl	Et
d	CH	2-thienyl	Et
e	CH	*p*-tolyl	Et
f	CH	3,5-diFPh	Et
g	N	Et	2-crotyl
h	N	Et	2-isopentenyl
i	N	Ph	Et
j	N	2-thienyl	Et
k	N	*m*-tolyl	Et

displayed by selected compounds and preliminary pharmacokinetic studies.

Chemistry

The pyrrolo[2,1-*d*][1,5]benzoxazepinones (PBOs) and pyrrolo[1,2-*d*]pyrido[3,2-*b*][1,5]oxazepinones (PPOs) **13a**−**k** were synthesized as shown in Scheme 1. Starting from the 1-(2−hydroxyphenyl)pyrrole **8**, previously described by Artico,[15] and from 1-(3-hydroxy-2-pyridyl)-pyrrole **9**, obtained starting from 2-amino-3-hydroxypyridine **7**, the esters **10a**−**i** were prepared by O-alkylation with the appropriate ethyl α-bromo esters (see refs 14 and 16a−c). Saponification of the ethyl ester group (NaOH, H_2O)[11a−i] followed by intramolecular cyclization using phosphorus pentachloride gave ketones **12a**−**j**. Treatment of the corresponding enolates with alkyl halides finally yielded the desired oxazepinones **13a**−**k**. The corresponding O-alkylated compounds were obtained as byproducts (10−25% yield).

Computer-Aided Design

The discovery of PBOs as a new class of NNRTIs prompted molecular modeling studies aimed at super-

Table 1. Inhibition of HIV-1wt and HIV-1 Mutant RT Enzymes, Containing the Single Amino Acid Substitutions L100I, K103N, V106A, Y181I, and Y188L

	K_i (μM)[a] polyrA(dT)$_{12-18}$					
compd	WT	L100I	K103N	V106A	Y181I	Y188L
6	0.19	0.75	7.7	3.9	>10	>10
13a	0.10	0.16	0.07	0.4	4	1.5
13b	0.06	0.011	0.022	0.01	>10	>10
13c	0.07	0.1	1.1	0.25	4	1.9
13d	0.03	0.07	0.4	0.11	0.97	0.3
13e	0.97	NT	NT	NT	NT	NT
13f	1.5	1.7	2.7	3.0	6.8	>10
13g	NA	NT	NT	NT	NT	NT
13h	NA	NT	NT	NT	NT	NT
13i	0.022	0.04	0.3	0.07	4	1.5
13j	0.093	0.09	0.045	0.09	0.43	0.475
13k	0.021	0.044	0.03	0.4	1.2	1.5
nevirapine	0.4	9	7	10	36	18

[a] Inhibition of HIV-1 RT activities. All the data listed were compared to the corresponding test results for nevirapine, performed at the same time. Each value is the mean of at least three experiments. NT, not tested; NA, not active, inhibition ≤10% at 10 μM final drug.

imposing the lead compound **6** on nevirapine as it is found in its crystallographic complex with RT.[17] It was felt that a pharmacophore-consistent alignment of these two compounds would facilitate the derivation of a model of the RT/**6** complex and subsequent structure-based design of novel inhibitors. We have recently proposed[14] that **6** binds in a conformation featuring the pendant phenyl ring in an equatorial disposition. Since both enantiomers of **6** (assayed as racemic mixture) were superimposable on nevirapine in a "butterfly-like" arrangement (Figure 1) we could not single out the preferred configuration of this compound. The pharmacophore-based conformations of *S*-**6** and *R*-**6** were each in turn placed into the non-nucleoside binding site (NNBS) extracted from the crystal structure of RT/nevirapine complex[17] to yield the corresponding complexes of NNBS/*S*-**6** and NNBS/*R*-**6** shown in Figure 2.

The following features of the two docking models are worthy to be outlined. The pendant phenyl (fused-pyrrole) ring of *S*-**6** (*R*-**6**) is embedded within a hydrophic pocket made up by the side chains of Pro95, Tyr181, Tyr188, Trp229, Leu100, and Leu234. The pyrrole (phenyl) moiety is surrounded by backbone atoms of His235, Pro236, Asp237, Lys101, and Lys102 and by side chains of Leu100, Lys103, and Val106. The ethyl group projects toward Val179 and Gly190 backbone. No intermolecular hydrogen bonds involve the oxygens of the ligand. The fused-benzene ring of both enantiomers extends to the NNBS entrance delimited by Glu138, Val179, Lys101, and Lys103 side chains. To roughly estimate the degree of steric complementarity between the docked ligand and the protein, we calculated the volume wherein the two partners of the complex overlap (OVOL). The higher OVOL the lower is the enzyme/inhibitor shape complementarity. This volume is linked to steric conflicts that can be potentially relieved by molecular dynamics and geometry optimization. The OVOLs associated with the NNBS/*S*-**6** and NNBS/*R*-**6** complexes (red contours in Figure 2) were not sufficiently dissimilar (13 and 4 Å^3, respectively) so as to conclude that only one complex (enantiomer) had biological relevance. Indeed, predicting differences in potency between the two enantiomers of **6** through computer intensive methods would have still left unsolved the question of which could be the preferred configuration for each designed virtual compound. Thus, both NNBS/*R*-**6** and NNBS/*S*-**6** complexes were analyzed as though the binding modes of the enantiomers of **6** had the same probability to occur. Inspection of the NNBS/*S*-**6** complex revealed room within the NNBS that could be filled by a small-size substituent inserted at the meta-position of the phenyl ring. Such a substituent was expected to occupy the NNBS pocket which accommodates the methyl group of nevirapine. Interestingly, a meta-substituent should be tolerated also on the pendant phenyl of the *R*-enantiomer because it would fit into the NNBS locus hosting the chlorine of 9-Cl-TIBO[18] and the proxymal part of the CH_2OCH_2-CH_2OH side chain of HEPT.[19] Accordingly, the *m*-tolyl and *m*-methoxyphenyl derivatives **13b** and **13c** were proposed for synthesis. To validate our model, we predicted that the *p*-tolyl derivative **13e** would result less active than its isomer **13c** because (i) Tyr181 and the Trp229 aromatic rings restrict the space accessible by the *p*-methyl in the *S*-enantiomer and (ii) the *p*-methyl in the *R*-enantiomer would collide with the carbonyl atoms of His235 and Pro236. Since the Tyr181 side chain appeared in a suitable orientation for a π-stacking interaction with the phenyl of *S*-**6**, electron-withdrawing groups introduced on this ring as well as its replacement with a more electron-deficient heteroaromatic ring (i.e. a thiophene[20]) were modifications expected to promote a putative charge-transfer interactions between the rings. Therefore, we planned the synthesis of **13a**, **13d**, and **13f**.

Further lead optimizations attempts assumed that the fused-benzene ring is not a pharmacophore element and that it may slightly worsen the steric match of both *R*- and *S*-enantiomers with the NNBS. Particularly, the OVOL calculated on the NNBS/*S*-**6** complex is essentially related to overlap of the fused-benzene ring C-1 and C-2 hydrogens with the Lys101 carbonyl and the Lys103 side chain atoms. Most of the OVOL associated with the NNBS/*R*-**6** complex is due to steric conflicts between the fused-benzene ring C-1 hydrogen and the Tyr181 side chain. The possibility to remove the fused-benzene was discarded owing to exceeding synthetic difficulties. A more feasible modification to reduce steric bulk at position 1 was the isosteric replacement of the fused-benzene 1-CH with a nitrogen, to give the PPO **13i**. The pendant phenyl ring of **13i** was replaced by a 2-crotyl or a 2-isopentenyl to yield compound **13g** or **13h**, respectively. The likelihood for these 6-alkenyl derivatives to elicit inhibitory activity was strongly supported by the finding that in the PBO series changing the phenyl to a 2-isopentenyl produced an inhibitor as active as the lead **6**.[14] Moreover, X-ray crystallographic experiments have shown that the 2-isopentenyl chain in 8-Cl-TIBO[21] and 9-Cl-TIBO[18] fills the same locus of the enzyme hosting the nevirapine A ring. Compounds **13j** and **13k** were prepared shortly after the biological assays on **13c**, **13d**, and **13i** and showed improved activities over the lead **6**. It was hoped, in fact, that combining structural features beneficial to activity, i.e., a *m*-tolyl or a 2-thienyl at position 6 with 1-CH/N replacement, would synergistically increase the inhibitory potency.

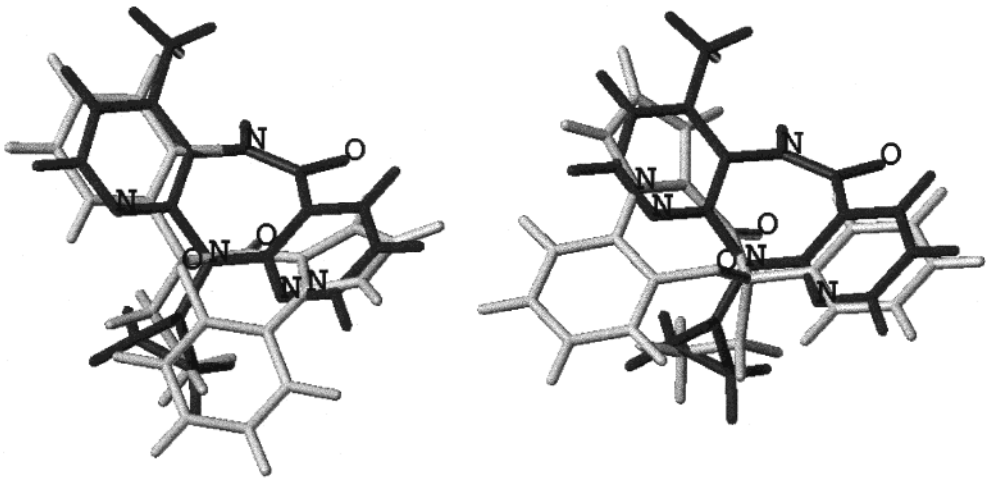

Figure 1. Overlay of the phenyl equatorial conformation of *S*-**6** (left) and *R*-**6** (right) on the RT-bound conformation of nevirapine.[17] The pendant phenyl and the fused-pyrrole rings of *S*-**6** match the pyridine A and C rings of nevirapine, respectively. The fitting of the aromatic rings is inverted for *R*-**6**. In both alignments the ethyl group is superimposed on the cyclopropyl ring of nevirapine. Compound **6** and nevirapine are depicted in light and dark gray, respectively.

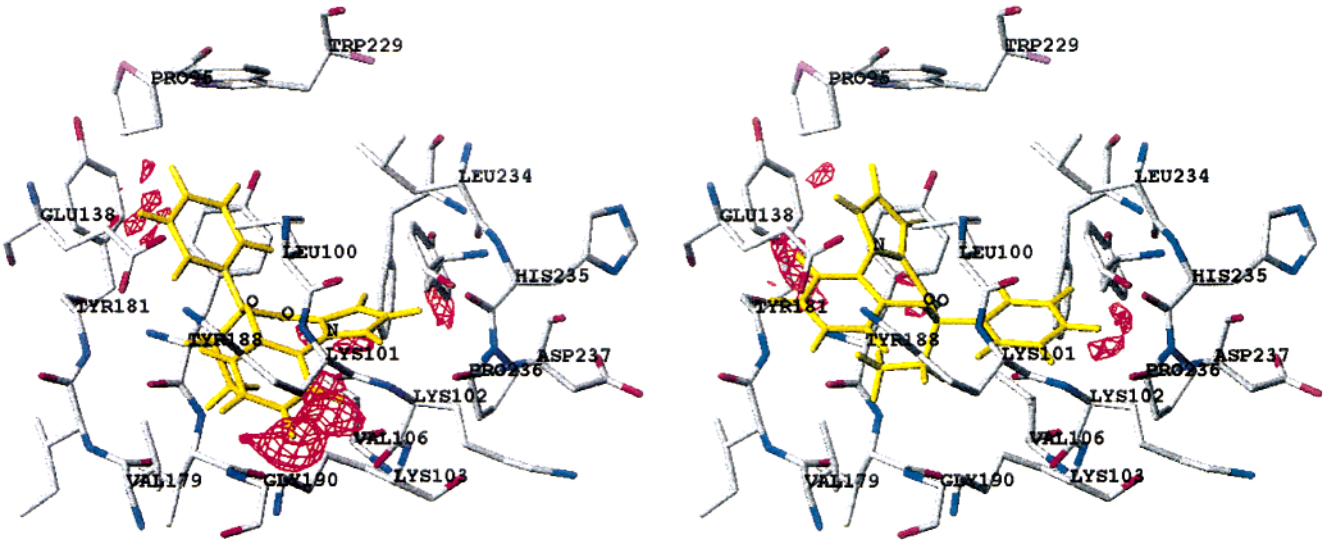

Figure 2. NNBS/*S*-**6** (left) and NNBS/*R*-**6** (right) complexes obtained by replacing nevirapine with the pharmacophore-based conformations of *S*-**6** and *R*-**6**. Only a subset of residues of the NNBS is displayed for sake of clarity. Red mesh contours delimit the overlap volume (OVOL) obtained by intersecting the ligand and the protein volumes.

Results and Discussion

Primary Tests. Antienzymatic Assays. All the new compounds described were tested in vitro against RTwt and several mutant RTs containing the single amino acid substitutions L100I, K103N, V106A, Y181I, and Y188L, known to confer NNRTI resistance in treated patients. The results are summarized in Table 2 as K_i values. Most of the compounds showed improved efficacy on RTwt with respect to the lead **6**. Particularly, the gain of potency obtained through **13a**−**d,i**−**k** varied from 2- to 9-fold. The *p*-tolyl derivative **13e** was found 14-fold less active than the *m*-tolyl isomer **13c** in accordance with our theoretical model. Contrary to our expectations, **13f**−**h** were devoid of appreciable activity. Inactivity of the 2-crotyl and 2-isopentenyl derivatives **13g** and **13h** suggests that their 2-alkenyl chains are not oriented similarly to the 2-isopentenyl group of TIBO inhibitors within the NNBS,[18,21] thus supporting the hypothesis that active PPOs bind preferentially as *R*-enantiomers (similarly to *R*-**6** on the right in Figure 1). Conversely, the fused-benzene isoster of **13h** resulted as active as **6** in our previous work.[14] It is worth outlining that insertion of a *m*-methyl on the phenyl ring (so as to mimic the methyl group in nevirapine) improves activity in the PBO series (compare **13c** vs **6**) but is irrelevant in the PPO series (compare **13k** vs **13i**). Taken together, these data suggest that PBOs can bind as *S*-enantiomers (Figure 1 on the left). As stated, **13j** and **13k** were designed by combining features favorable for activity, i.e. the *m*-tolyl in **13c**, the 2-thienyl in **13d**, and the fused-pyrido ring in **13i**. Although more potent than the lead **6**, these two "hybrids" did not however exhibit synergistically increased efficacies resulting from additive effects of structural modifications. If we admit that the active configuration/binding mode of PBOs and PPOs is dictated by the overall stereoelectronic properties of each ligand, we can also explain why **13j** and **13k** were not so active as expected. In fact, if the nevirapine A ring is mimicked by the aryl rings of **13c** and **13d** (binding as *S*-enantiomers) as well as by the fused pyridine ring of **13i** (binding as *R*-enantiomer), none of the enantiomers of **13j** and **13k** can obviously

Table 2. Inhibition of HIV-1 Infection in CEM-SS Cells,[a] Inhibition of HIV-IIIB Infection in C8166 Cells, and Cytotoxicity on NSO Murine Cell Line, Daudi Human (DH) Cell Line, 3T3 Fibroblasts (3T3F) Murine Cell Line, and Normal Human Lymphocytes (HL)

	CEM-SS cells			C8166 cells			TC_{50} (mM)[e]			
compd	IC_{50} (μM)[b]	EC_{50} (μM)[c]	SI[d]	IC_{50} (μM)[b]	EC_{50} (μM)[c]	SI[d]	NSO[f]	DH[g]	3T3F[h]	HL[i]
6j	4.9	0.47	11	10	0.8	12.5	0.024	0.026	0.033	0.032
13a	2.0	0.072	28	13.8	1.1	12.7	0.72	0.72	0.71	0.72
13b	0.2	0.04	5	7.0	0.033	212	0.23	0.28	0.21	0.2
13c	119	0.35	338	52	0.425	122	>1	>1	>1	>1
13d	11	0.115	95	NT	NT	NT	NT	NT	NT	NT
13f	NT	NT	NT	17.1	0.65	26	NT	NT	NT	NT
13i	3.9	0.069	56	6.0	0.054	111	0.014	0.013	0.01	0.013
13j	>2.0	0.15	>13	20.5	1.2	16.6	0.026	0.029	0.035	0.030
13k	>2.0	0.027	>75	7.2	0.27	26.7	0.41	0.38	0.40	0.40
AZT	>1	0.0019	526	>100	0.4	>250				

[a] Testing was performed by the National Cancer Institute's Developmental Therapeutics Program, AIDS Antiviral Screening Program. All the data listed were compared to the corresponding test results for AZT which served as the treated control, performed at the same time. [b] The IC50 value is the test drug concentration which results in a 50% survival of uninfected untreated control CEM-SS cells (e.g. cytotoxicity of the test drug) or macrophages cells (C8166). [c] The EC50 value is the test drug concentration which produces a 50% survival of HIV-1-infected cells relative to uninfected untreated controls (e.g. in vitro anti-HIV-1 activity). [d] SI, selectivity index (IC_{50}/EC_{50}). [e] Blank was subtracted from OD measured at 570 nm. All data reported are measured OD × 1000. Standard deviations are not reported but never exceed 5% of the mean value. [f] OD measured in control row was 0.125 ± 0.015. [g] OD measured in control row was 0.129 ± 0.018. [h] OD measured in control row was 0.131 ± 0.014. [i] OD measured in control row was 0.114 ± 0.01. [j] Reference 14. NT, not tested.

Table 3. EC_{50} and Combination Index (CI) for the Anti-HIV-1 Compounds **13c** and **13i** in Association with AZT, Calculated Using Both the Mutually Nonexclusive and the Mutually Exclusive Assumptions[a]

	EC_{50} (nM)			CI[b]	
compd	of compounds alone	of compounds with AZT	of AZT with compounds	mutually exclusive assumption	mutually nonexclusive assumption
none			400		
13c	425	11	3.25	0.040	0.040
13i	54	17	3.17	0.302	0.303

[a] C8166 cells were infected with HIV−IIIB. [b] CI > 1, CI = 1, and CI < 1 indicate antagonistic, additive, and synergistic activities, respectively. The CI values were calculated at 50% antiviral activity using both the mutually nonexclusive and the mutually exclusive forms of the equation.

position both favorable aromatic moieties into the same NNBS region. With respect to our lead **6**, the PBOs **13a**−**c** and the PPO **13i** were found much more active against L100I, K103N, and V106A mutants. Of particular interest was the submicromolar potency elicited by the 6-(2−thienyl) derivatives **13d** and **13j** against all the considered mutant RTs. Mager has proposed that conformational flexibility and overall size of the inhibitor are the main determinants of binding affinity to mutant forms of RT.[22] Molecular mechanics calculations performed in our laboratories revealed that the 2-thienyl ring at the 6-position in compound **13d** is more free to rotate about the C-6−C-1′ bond compared with the corresponding phenyl ring in **6** (unpublished observations). The remarkable performance of **13d** and **13j** might depend on a greater capability to adapt their conformation to changes in the shape of the NNBS resulting from a single mutation.

Secondary Tests. A subset of compounds with promising antienzymatic profile in primary screening was further evaluated for in vitro antiviral activity on lymphocytes and monocyte-macrophages (Table 2), for cytotoxicity on a panel of cell lines (Table 2), and for potential synergistic antiviral activity with AZT (Table 3).

1. Cell Culture Assays. On the CEM-SS cell line (Table 2), **13c** resulted practically equipotent, whereas the remaining selected compounds (**13a**−**d,i**−**k**) turned out to be more active compared with the lead **6** (**13b** and **13k** by 12- and 17-fold, respectively). The better antiviral properties of the newly synthesized compounds were confirmed on C8166 cells infected with HIV-III Ba-L (Table 2), except for **13a**, whose activity was found slightly lower than that of **6**.[23] Remarkably, **13b** and **13i** showed 24- and 14-fold improvement of potency over **6**. Testing of **13c** and **13i** on monocyte-macrophages characterized these compounds as promising antiviral agents in terms of efficacy (EC_{50} values of 42 and 43 nM, respectively) and low cytotoxicity (SI values of 826 and >46, respectively).

2. MTT Assays. To confirm the low cytotoxicity data shown in cell culture assays, compounds **13a**−**c,i**−**k** were further screened in a MTT assay by using NSO murine, Daudi human, and 3T3 fibroblast murine cell lines and normal human lymphocytes (Table 2). In these tests, the title compounds showed low toxicity, with the exception of **13i** and **13j** whose toxicity is in the micromolar range and is comparable with that exhibited by the lead **6**. Compound **16c** stands out for its extremely low cytotoxicity (TC_{50} values > 1 mM).

3. Synergistic Antiviral Activity with AZT. The recent therapeutic developments of AIDS converge to favor multidrug regimens which have shown to improve the chances of success. A further improvement in multidrug therapy would be to administer combinations of drugs able to interact synergistically. This so-called "second level" of combinations consists of drugs acting at different sites within the same viral protein.[24] According to this approach, we decided to investigate the synergistic antiviral activity of our NNRTIs, with AZT (NRTI). Two of the most active compounds (**13c**, **13i**) showed synergistic anti-HIV-1 activity (CI <1) when tested in combination with AZT, whether the mutually exclusive or nonexclusive assumption formulas were used (Table 3).

Pharmacokinetic Studies. Initial pharmacokinetic studies were done on compounds **13b** and **13c**. Only trace amounts of the unchanged compounds were detectable in whole brain (not in blood or plasma) within 60 min of oral dosing to mice (10−20 mg/kg, suspended in 10% Tween 80 in water). This may be referred to an incomplete absorption and/or an extensive first-pass effect as a result of the water insolubility of these compounds and their high lipophilicity. The log *P* values calculated for **13b** and **13c** were 4.95 and 5.53, respectively (see Experimental Section). After subcutaneous injection (20 mg/kg) the two derivatives were measurable in whole brain (and trace amounts of **13b** were also detectable in plasma), but the concentrations were relatively low and variable, particularly for the more lipophilic **13c**. The mean brain maximum concentrations (observed 30 min after dosing) approximated 0.5 nmol/g for **13c** and 1.2 nmol/g for **13b**, with coefficients of variation approaching respectively 90% and 50%.[25]

Pharmacokinetic studies were successively extended to **13i**. This PPO derivative is less lipophilic (calculated log *P* value 4.05) than **13b**, as also indicated by the different elution characteristics (see Experimental Section). When given to mice orally (20 mg/kg), as a solution in 10% Tween 80−5% ethanol in HCl, 10^{-3} M, it rapidly reached the systemic circulation, although mean C_{max} (0.6 nmol/mL, 15 min after dosing) and AUC_t were only about 30% of those after the same dose subcutaneously. This compound also showed good brain penetration, with brain C_{max} (8.0 ± 1.7 nmol/g, 15 min after subcutaneous dosing) and AUC (542 nmol/g min) about 4 times the corresponding plasma values (2.1 nmol/mL and 141 nmol/mL min). Its elimination $t_{1/2}$ was calculated from the 0.5−3 h time points of the subcutaneous plasma and brain profiles and was about 65 min in both tissues.[26]

Conclusions

With the goal to develop more potent and broad-spectrum analogues within the series of oxazepinone RT inhibitors, we investigated several structural features for conferring optimum enzyme inhibition. Focusing directly on a small number of structural alterations, dictated by docking studies, we have been able to identify analogues of **6** with a greatly improved pharmacological profile, in terms of efficacy, broad spectrum, and low cytotoxicity. The antiviral activity and the synergistic antiviral properties with AZT suggest a potential clinical utility of analogues such as **13b**−**d**, **13i**, and **13j**, in combination with NRTIs, against strains of HIV-1 bearing those mutations that confer resistance to the known NNRTIs.

Experimental Section

For general experimental information, see ref 14. The α-bromo esters used for the synthesis of compounds **10a**−**i** were synthesized by halogenation with *N*-bromosuccinimide of the corresponding arylacetic acid ethyl esters, by using a synthetic procedure described in refs 14 and 16, except for α-bromobutyric acid ethyl ester which was purchased from Aldrich.

1-(3-Hydroxy-2-pyridyl)pyrrole (9). To a solution of 2-amino-3-hydroxypyridine (**7**) (7.5 g, 68.1 mmol) in 250 mL of glacial acetic acid, heated at 95−100 °C, was added 2,5-dimethoxytetrahydrofuran (9.0 g, 68.1 mmol) in glacial acetic acid (20 mL). The mixture was stirred for 30 min, the solvent was removed in vacuo, and the residue was extracted with EtOAc. The organic layers were washed with 5% $NaHCO_3$ solution and brine, dried, and evaporated. The crude product was purified by silica gel column chromatography using dichloromethane/ethyl acetate (8:2) as eluant. Fractions containing the product were combined, dried, and recrystallized by ethyl ether to give analytically pure **9** (4.7 g) as white prisms: IR (KBr) 2928 cm^{-1}; ^1H NMR (CD_3OD) δ 6.08 (m, 2 H), 6.96 (dd, 1 H, J = 7.9, 4.6 Hz), 7.21 (d, 1 H, J = 7.9 Hz), 7.42 (m, 2 H), 7.75 (d, 1H, J = 4.6 Hz). Anal. ($C_9H_8N_2O$) C, H, N.

General Procedure for Preparation of Compounds 10a−i. This procedure is illustrated for the preparation of (±)-α-[[2-(1*H*-pyrrol-1-yl)phenyl]oxy](*m*-fluorophenyl)acetic acid ethyl ester (**10a**). Sodium hydride (347 mg, 14.4 mmol) was added to a solution of 1-(2−hydroxyphenyl)pyrrole (2.1 g, 13.1 mmol) in anhydrous THF at room temperature. The reaction mixture was stirred for 1 h at room temperature, and then a solution of ethyl α-bromo-*m*-fluorophenylacetate (3.0 g, 13.1 mmol) in anhydrous THF (20 mL) was added dropwise. After 16 h at room temperature, the solvent was removed in vacuo, and the residue was taken up in dichloromethane. The organic layer was washed with brine, dried, and concentrated. The residue was purified by flash chromatography (dichloromethane/hexanes, 2:1) to give **10a** as a colorless oil: IR (neat) 1748 cm^{-1}; ^1H NMR ($CDCl_3$) δ 7.21 (m, 10 H), 6.42 (m, 2 H), 5.58 (s, 1 H), 4.21 (q, 2 H, J = 7.6 Hz), 1.22 (t, 3 H, J = 7.7 Hz). Anal. ($C_{20}H_{18}FNO_3$) C, H, N.

General Procedure for Preparation of Compounds 11a−i. This procedure is illustrated for the preparation of (±)-α-[[2-(1*H*-pyrrol-1-yl)phenyl]oxy](*m*-fluorophenyl)acetic acid (**11a**). The ester **10a** (1.0 g, 29 mmol) was dissolved in 10 mL of EtOH and 5% aqueous NaOH was added. The reaction mixture was stirred at room temperature for 17 h, concentrated, and acidified with 1 N HCl. The aqueous phase was extracted with EtOAc, and the organic layer was washed with brine, dried, and concentrated. The residue was recrystallized to give the acid **11a** as colorless prisms: IR (Nujol) 1745 cm^{-1}; ^1H NMR ($CDCl_3$) δ 9.31 (br, s, 1 H), 7.17 (m, 10 H), 6.34 (m, 2 H), 5.49 (s, 1 H). Anal. ($C_{18}H_{14}FNO_3$) C,H,N.

General Procedure for Preparation of Oxazepinones 12a−d,f−j. This procedures is illustrated for the preparation of (±)-6-(*m*-fluorophenyl)pyrrolo[2,1-*d*][1,5]benzoxazepin-7(6*H*)-one (**12a**). Phosphorus pentachloride (0.55 g, 2.3 mmol) was added to a solution of acid **11a** (0.64 g, 2.06 mmol) within 20 min. The reaction mixture was stirred at room temperature for 5 h and then was poured into crushed ice, basified with 10% NaOH solution, and extracted with chloroform. The organic layers were washed with brine, dried, and evaporated. The residue was purified by flash chromatography (dichloromethane) and recrystallized (hexanes). The title compound was obtained as colorless prisms: IR (Nujol) 1741 cm^{-1}; ^1H NMR ($CDCl_3$) δ 7.20 (m, 10 H), 6.49 (m, 1 H), 5.47 (s, 1 H). Anal. ($C_{18}H_{12}FNO_2$) C,H,N.

General Procedure for Preparation of Compounds 13a−k. This procedure is illustrated for the preparation of (±)-6-ethyl-6-(*m*-fluorophenyl)pyrrolo[2,1-*d*][1,5]benzoxazepin-7(6*H*)-one (**13a**). A solution of **12a** (0.42 g, 1.43 mmol) in anhydrous THF (2.6 mL) was added to a suspension of potassium hydride (183 mg, 1.6 mmol, 35% in oil). The reaction mixture was stirred for 1.5 h at room temperature, and then ethyl iodide (231 mL, 2.9 mmol) was added. After an additional 15 h at room temperature the solvent was removed, and the residue was extracted with dichloromethane. The organic layers were washed with brine, dried, and evaporated. The residue was purified by flash chromatography (chloroform and hexanes, 1/1) and recrystallized to give **13a** as colorless prisms: IR (Nujol) 1697 cm^{-1}; ^1H NMR ($CDCl_3$) δ 7.08 (m, 10 H), 6.44 (m, 1 H), 2.34 (m, 2 H), 1.00 (t, 3 H, J = 7.5 Hz). Anal. ($C_{20}H_{16}FNO_2$) C,H,N.

Molecular Modeling. Molecular modeling studies were performed using the SYBYL program[27] running on a Silicon Graphics Iris Indigo XS24 workstation. The crystal structure of the RT/nevirapine complex solved at 2.2 Å resolution by Ren

et al.[17] was retrieved from the Brookhaven Protein Data Bank[28] (entry code 1VRT). Nevirapine and the NNBS, this latter consisting of a set of amino acids located within 10 Å from any non-hydrogen atom of the bound inhibitor, were extracted from the complex. Water molecules were deleted, and hydrogens were added to the unfilled valences of the amino acids. Nevirapine was removed, and the pharmacophore-based conformations of *S*-**6** and *R*-**6** were each in turn placed into the NNBS to yield the corresponding complexes of NNBS/*S*-**6** and NNBS/*R*-**6**. Modeling of **6** and its alignment on nevirapine are described in a previous study.[14] Manipulation and display of molecular volumes were realized with the MVOLUME command of SYBYL. Semiempirical quantum-mechanics calculations of benzene and thiophene LUMO energies were performed using the AM129 and PM330 Hamiltonians available in the MOPAC program (version 6.0, QCPE, Indiana University, Bloomington, IN) under default settings. The calculated *n*-octanol/water log *P* values for compounds **13b**, **13c**, and **13i** were obtained running the ClogP program (version 2.0, Biobyte Corp., Claremont, CA).

HIV-1 RT RNA-Dependent DNA Polymerase Activity Assay. RNA-dependent DNA polymerase activity assay was assayed as follows: a final volume of 25 μM contained reaction buffer (50 mM Tris-HCl, pH 7.5, 1 mM DTT, 0.2 mg/mL BSA, 4% glycerol), 10 mM $MgCl_2$, 0.5 μg of poly(rA):oligo(dT)$_{10:1}$ (0.3 μM 3′-OH ends), 10 μM [^{3}H]dTTP (1 Ci/mmol), and 2−4 nM RT. Reactions were incubated at 37 °C for the indicated time; 20-μL aliquots were then spotted on glass fiber filters GF/C which were immediately immersed in 5% ice-cold TCA. Filters were washed twice in 5% ice-cold TCA and once in ethanol for 5 min and dried, and acid-precipitable radioactivity was quantitated by scintillation counting.[31]

Inhibition Assay. Reactions were performed under the conditions described for the HIV-1 RT RNA-dependent DNA polymerase activity assay. Incorporation of radioactive dTTP into poly(rA):oligo(dT) was monitored in the presence of increasing amounts of the inhibitors to be tested. Data were then plotted according to Lineweaver−Burke and Dixon. For K_i determinations an interval of inhibitor concentrations between 0.2 K_i and 5 K_i was used. Experiments have been done in triplicate. Experimental errors (±SD) were ≤10%.

In Vitro Anti-HIV Assays. Cell Culture Assay. 1. CEM Cell Line. The ability of the test compounds to protect HIV-1-infected T4 lymphocytes (CEM cells) from cell death was determined following the reported procedure.[32] All compounds were compared with a positive (AZT-treated) control performed at the same time under identical conditions.

2. Other Cells. Mature macrophages were obtained by incubating in 48-well plates (Costar, Cambridge, MA) 10^6 PBMC/mL of complete medium (containing Roswell Park Memorial Institute (RPMI)-1640, penicillin 100 units/mL, streptomycin 100 mg/mL, L-glutamine 0.3 mg/mL, and 20% heat-inactivated fetal calf serum). After 7 days of incubation in 5% CO_2 at 37 °C, nonadherent cells (lymphocytes) were removed by extensive washing. Using this method, the yield, after removal of the nonadherent cells, was 10^5 macrophages/well. Further details of this procedure are described elsewhere.[33] Macrophages obtained with this method are >95% pure as detected by nonspecific esterase activity. C8166 is a CD4$^+$ T-cell line containing an HTLV-I genome of which only the *tat* gene is expressed.[34]

3. Virus. A laboratory, lymphocyte-tropic strain of HIV-1 (HIV-1-IIIB) was used to infect C8166. A laboratory monocyte-tropic strain of HIV-1 (HTLV-III Ba-L, also called HIV Ba-L) was used to infect macrophages. Details of the characteristics of the laboratory strain are reported elsewhere.[35,36] The sources of the HIV-1 laboratory lymphocyte-tropic and monocyte-tropic strains were respectively the supernatants of H9/IIIB (H9) cultures (H9 is a CD4$^+$ T-cell line persistently infected with HIV-1)[35] and the supernatants of infected macrophages cultures. Titration to determine the infectivity was performed in human macrophages as previously described. The titer of the virus stocks, expressed as 50% tissue culture infectious dose ($TCID_{50}$), was determined as previously described.[37]

4. Antiviral Agent. Zidovudine (AZT) was purchased from Sigma Chimica.

5. Toxicity. Chemicals toxicity in C8166 was evaluated with a procedure involving a colorimetric assay (MTT assay) that monitors the ability of viable, but not dead, cells to reduce 3-(4-dimethylthiazol-2-yl)-2,5-diphenyltetrazolium bromide (MTT) to a blue formazan product, which can be measured spectrophotometrically. Details of this methods are described elsewhere.[38,39]

6. Assay of Antiviral Activity. For evaluation of antiviral activity in acutely infected C8166 cultures, the cells were distributed into 15-mL polyethylene tubes at a concentration of 90×10^3 cells/mL and exposed to 100 $TCID_{50}$ of HIV in the presence or absence of antiviral compounds. After 2 h incubation in 5% CO_2 at 37 °C the cells were washed twice in PBS and inoculated in each well of a 96-well plate (Falcon 3042, Falcon, Basel, Switzerland) at a concentration of 35×10^3 cells/200 μL of complete medium. The cells were subsequently cultured in the presence of the same concentrations of drugs as before for 5 days. The antiviral activity of the compounds was assessed by quantifying the HIV-induced cytopathogenicity by the MTT assay. The percentage of protection from the cytopathic effect achieved by each compound in HIV-infected cells measured by the MTT assay was calculated by the following formula: $(OD_T)_{HIV} - (OD_C)_{HIV}/(OD_C)_{mock} - (OD_C)_{HIV}$, expressed in %, whereby $(OD_T)_{HIV}$ is the optical density measured with a given concentration of compound in HIV-infected cells, $(OD_C)_{HIV}$ is the optical density measured for the control untreated HIV infected cells, and $(OD_C)_{mock}$ is the optical density measured for the control untreated mock infected cells. The optical density at 490/650 nm was measured using a plate reader. The assay to evaluate anti-HIV drug efficacy in acutely infected mature macrophages has been previously described.[33] The antiviral activity of the compounds was assessed by measuring HIV-p24 antigen production in the supernatants of infected cultures as previously described[35] by using a commercially available HIV-antigen kit.

7. Immunofluorescence Virus Binding Assay. Calculation of the 50% effective dose (ED_{50}) and 50% inhibitory dose (ID_{50}) was done from pooled values in the effective dynamic range of the antiviral and toxicity assays (5−95%) using the median effect equation as previously described.[40]

Toxicity Tests. 1. Cell Lines. All cell lines were obtained from ATCC. The cells were cultured in RPMI-1640 supplemented with 5% FCS, 0.1 mM glutamine, 1% penicillin, and streptomycin. Cells were grown in Nunc clone plastic bottles (TedNunc, Roskilde, Denmark) and split twice weekly at different cell densities according to standard procedure. 3T3 cells were grown as monolayer and split by using trypsin. Peripheral blood mononuclear cells (MNC) were separated from heparinized whole blood obtained from a healthy donor on a Fycoll-Hypaque gradient as previously described.[41] MNC thus obtained were washed twice with RPMI-1640 supplemented with 10% FCS, glutamine, and antibiotics, suspended at 200 000 viable cells/mL in medium containing, as mitogen, 5 μg/mL PHA (Sigma), and used in toxicity tests.

2. Chemicals. MTT was purchased from Aldrich. It was dissolved at a concentration of 5 mg/mL in sterile PBS at room temperature, and the solution was further sterilized by filtration and stored at 4 °C in a dark bottle. SDS was obtained from Sigma. Lysis buffer was prepared as follows: 20% w/v of SDS was dissolved at 37 °C in a solution of 50% of each DMF and demineralized water; pH was adjusted to 4.7 by adding 2.5% of an 80% acetic acid and 2.5% 1 N HCl solution.

3. Toxicity Experiments. Cells were plated at different concentrations on flat-bottom 96-well microplates (0.1 mL/well). Lymphocytes were plated out at 20 000 cells/well. 3T3 cells (murine fibroblast line) were plated at 10 000 cells/well. NSO cells (plasmocytoma murine cell line) were plated out at 3 000 cells/well, and Daudi cells (human lymphoblastoid cell line) were plated at 300 cells/well. 12 h after plating, different concentrations of each compound were added to each well. After 48 h, MTT assay was performed to analyze cytotoxicity of the different compounds. Some experiments were performed

by using confluent cells: compounds were added to 3T3 monolayer 3 days after plating. Tests were then run as described above.

4. MTT/Formazan Extraction Procedure. 20 μL of the 5 mg/mL stock solution of MTT was added to each well; after 2 h of incubation at 37 °C, 100 μL of the extraction buffer was added. After an overnight incubation at 37 °C, the optical densities at 570 nm were measured using a Titer-Tech 96-well multiscanner, employing the extraction buffer as the blank.

Synergy Calculations. The multiple drug effect analysis of Chou and Talalay[42] was used to calculate combined drug effects.

Drug Administration and Plasma and Brain Sampling. Male CD1 mice weighing about 25 g (Charles River, Italy) were used. Procedures involving animals and their care were conducted in conformity with the institutional guidelines that are in compliance with national laws (D.L. n. 116, G.U., Suppl. 40, Feb 18, 1992; Circolare No. 8, G.U., 1994) and international laws and policies (EEC Council Directive 86/609, OJ L 358,1, Dec 12, 1987; *Guide for the Care and Use of Laboratory Animals*, U.S. National Research Council, 1996). Mice received the test compounds orally (suspended in 10% Tween 80 in water) and subcutaneously (10% Tween 80 in water or 10% Tween 80−5% ethanol in 10^{-3} M hydrochloric acid) at doses of 10−20 mg/kg and were killed by decapitation under deep anesthesia at various times after dosing. Blood samples were collected in heparinized tubes and centrifuged and the plasma was stored at −20 °C. Brains were rapidly removed, blotted with paper to remove excess surface blood, and stored at −20 °C until analysis.

Drug Analysis. Plasma and brain concentrations of the test compounds were determined by high-performance liquid chromatography (HPLC) after a liquid−liquid extraction procedure. A chromatographically suitable analogue with similar extraction characteristics was used as internal standard (IS) in each assay.

Acknowledgment. We are grateful to the Istituto Superiore di Sanita', Italy, for financial support (Progetto Patologia, Clinica e Terapia dell' AIDS, Grant 30A/0/44). This work has also been supported by the CNR Target Project on Biotechnology (to S.S.) and by the ISS-AIDS Fellowship (to G.M.). We also thank Claudia Fracasso for expert technical assistance. Giuseppe Caliendo thanks Assessorato Ricerca Scientifica - Regione Campania, Italy (POP 5.4.2).

Supporting Information Available: Experimental details relative to synthesis and physical and chemical data of compounds **10**−**13**, synergy calculations, and pharmacokinetic studies. This material is available free of charge via the Internet at http://pubs.acs.org.

References

(1) De Clercq, E. HIV Inhibitors Targeted at the Reverse Transcriptase. *AIDS Res. Hum. Retrovirus* **1992**, *8*, 119−134.
(2) Therapeutic Approaches to HIV. *Perspect. Drug Discovery Des.* **1993**, *1*, 1−250.
(3) (a) Powell, K. L.; Darby, G. HIV Reverse Transcriptase as a Target for Antiviral Drugs. In *Design of Anti-AIDS Drugs*; DeClercq, E., Ed.; Elsevier: New York, 1990; pp 123−140. (b) Goff, S. P. Retroviral reverse Transcriptase: Synthesis, Structure, and Function. *J. AIDS* **1990**, *3*, 817−831.
(4) Mitsuya, H.; Broder, S. Strategies for Antiviral Therapy in AIDS. *Nature* **1987**, *325*, 773−778.
(5) Young, S. D. Non-Nucleoside Inhibitors of HIV-1 Reverse Transcriptase. *Perspect. Drug Discovery Des.* **1993**, *1*, 181−192.
(6) Terasaki, T.; Pardridge, W. M. Restricted Transport of 3′-Azido-3′-deoxythymidine and Dideoxynucleosides Through the Blood-Brain Barrier. *J. Infect. Dis.* **1988**, *158*, 630−632.
(7) Kumar, R.; Wang, L.; Wiebe, L. I.; Knaus, E. E. Synthesis and Antiviral (HIV-1, HBV) Activities of 5-Halo-6-methoxy(or azido)-5,6-dihydro-3′-fluoro-3′-deoxythymidine Diastereomers. Potential Prodrugs to 3′-Fluoro-3′-deoxythymidine. *J. Med. Chem.* **1994**, *37*, 3554−3560.
(8) Richman, D. D. Resistance of Clinical Isolates of Human Immunodeficiency Virus to Antiretroviral Agents. *Antimicrob. Agents Chemother.* **1993**, *37*, 1207−1221.
(9) (a) Hargrave, K. D.; Proudfoot, J. R.; Grozinger, K. G.; Cullen, E.; Kapadia, S. R.; Patel, U. R.; Fuchs, V. U.; Mauldin, S. C.; Vitous, J.; Behnke, M. L.; Klunder, J. M.; Pal, K.; Skiles, J. W.; McNeil, D. W.; Rose, J. M.; Chow, G. C.; Skoog, M. T.; Wu, J. C.; Schmidt, G.; Engel, W. W.; Eberlein, W. G.; Saboe, T. D.; Campbell, S. J.; Rosenthal, A. S.; Adams, J. Novel Non-Nucleoside Inhibitors of HIV-1 Reverse Transcriptase. 1. Tricyclic Pyridobenzo- and Dipyridodiazepinones. *J. Med. Chem.* **1991**, *34*, 2231−2241 and references therein. (b) Cohen, K. A.; Hopkins, J.; Ingraham, R. H.; Pargellis, G.; Wu, J. C.; Palladino, D. E. H.; Kinkade, P.; Warren, T. C.; Rogers, S.; Adams, J.; Farina, P. R.; Grob, P. M. Characterization of the Binding Site of Nevirapine (BI−RG-587), a Non-Nucleoside Inhibitor of Human Immunodeficiency Virus Type-1 Reverse Transcriptase. *J. Biol. Chem.* **1991**, *266*, 14670−14674. (c) Klunder, J. M.; Hargrave, K. D.; West, M.; Cullen, E.; Pal, K.; Behnke, M. L.; Kapadia, S. R.; McNeil, D. W.; Wu, J. C.; Chow, G. C.; Adams, J. Novel Non-Nucleoside Inhibitors of HIV-1 Reverse Transcriptase. 2. Tricyclic Pyridobenzoxazepinones and Dibenzoxazepinones. *J. Med. Chem.* **1992**, *35*, 1887−1897.
(10) (a) Pauwels, R.; Andries, K.; Desmyter, J.; Schols, D.; Kukla, M. J.; Breslin, H. J.; Raeymaeckers, A.; Van Gelder, J.; Woestenborghs, R.; Heykants, J.; Schellekens, K.; Janssen, M. A. C.; De Clercq, E.; Janssen, P. A. J. Potent and Selective Inhibition of HIV-1 Replication In Vitro by a Novel Series of TIBO Derivatives. *Nature* **1990**, *343*, 470−474. (b) Breslin, H. J.; Kukla, M. J.; Ludovici, D. W.; Mohrbacher, R.; Ho, W.; Miranda, M.; Rodgers, J. D.; Hitchens, T. K.; Leo, G.; Gauthier, D. A.; Ho, C. Y.; Scott, M. K.; De Clercq, E.; Pauwels, R.; Andries, K.; Janssen, M. A. C.; Janssen, P. A. J. Synthesis and Anti-HIV-1 Activity of 4,5,6,7-Tetrahydro-5-methylimidazo[4,5,1-jk][1,4]-benzodiazepin-2(1H)-one (TIBO) Derivatives. *J. Med. Chem.* **1995**, *38*, 771−793.
(11) Cantrell, A. S.; Engelhardt, P.; Hogberg, M.; Jaskunas, S. R.; Johansson, N. G.; Jordan, C. L.; Kangasmetsa, J.; Kinnick, M. D.; Lind, P.; Morin, J. M. Jr.; Muesing, M. A.; Noreen, R.; Oberg, B.; Pranc, P.; Sahlberg, C.; Ternansky, R. J.; Vasileff, R. T.; Vrang, L.; West, S. J.; Zhang, H. Phenethylthiazolylthiourea (PETT) Compounds as a New Class of HIV-1 Reverse Transcriptase Inhibitors. 2. Synthesis and Further Structure−Activity Relationship Studies of PETT Analogues. *J. Med. Chem.* **1996**, *39*, 4261−4274.
(12) Goldman, M. E.; Nunberg, J. H.; O'Brien, J. A.; Quintero, J. C.; Schleif, W. A.; Freund, K. F.; Gaul, S. L.; Saari, W. S.: Wai, J. S.; Hoffman, J. M.; Anderson, P. S.; Hupe, D. J.; Emini, E. A.; Stern, A. M. Pyridone Derivatives: Specific Human Immunodeficiency Virus Type-1 Reverse Transcriptase Inhibitors with Antiviral Activity. *Proc. Natl. Acad. Sci. U.S.A.* **1991**, *88*, 6863−6867.
(13) (a) Sardana, V. V.; Emini, E. A.; Gotlib, L.; Graham, D. J.; Lineberger, J. A.; Long, W. J.; Schlabach A. J.; Wolfang, J. A.; Condra, J. H. Functional Analysis of HIV-1 Reverse Transcriptase Amino Acids Involved in Resistance to Multiple Non-Nucleoside Inhibitors. *J. Biol. Chem.* **1992**, *267*, 17526−17530. (b) Nunberg, J. H.; William, A. S.; Boots, E. J.; O'Brien, J. A.; Quintero, J. C.; Hoffman, J. M.; Emini, E. A.; Goldman, M. E. Viral Resistance to Human Immunodeficiency Virus Type 1-Specific Pyridinone Reverse Transcriptase Inhibitors. *J. Virol.* **1991**, *65*, 4887−4892. (c) De Clercq, E. Resistance to Reverse Transcriptase Inhibitors. *Biochem. Pharmacol.* **1994**, *47*, 155−169. (d) Tantillo, C.; Ding, J.; Jacobo-Molina, A.; Nanni, R. G.; Boyer, P. L.; Hughes, S. H.; Pauwels, R.; Andries, K.; Janssen, P. A. J.; Arnold, E. Locations of Anti-AIDS Drug Binding Sites and Resistance Mutations in the Three-Dimensional Structure of HIV-1 Reverse Transcriptase. *J. Mol. Biol.* **1994**, *243*, 369−387.
(14) Campiani, G.; Nacci, V.; Fiorini, I.; De Filippis, M. P.; Garofalo, A.; Greco, G.; Novellino, E.; Altamura, S.; Di Renzo, L. Pyrrolobenzothiazepinones and Pyrrolobenzoxazepinones: Novel and Specific Non-Nucleoside HIV-1 Reverse Transcriptase Inhibitors with Antiviral Activity. *J. Med. Chem.* **1996**, *39*, 2672−2680.
(15) Artico, M.; Porretta, G. C.; De Martino, G. Synthesis of 4H−Pyrrolo[2,1-c][1,4]benzoxazine. *J. Heterocycl. Chem.* **1971**, *8*, 283−287.
(16) (a) Fiorini, I.; Nacci, V.; Ciani, S. M.; Garofalo, A.; Campiani, G.; Savini, L.; Novellino, E.; Greco, G.; Bernasconi, P.; Mennini, T. Novel Ligands Specific for Mithocondrial Benzodiazepine Receptors: 6-Arylpyrrolo[2,1-d][1,5]benzothiazepine Derivatives. Synthesis, Structure−Activity Relationships, and Molecular Modeling Studies. *J. Med. Chem.* **1994**, *37*, 1427−1438 and references therein. (b) Campiani, G.; Nacci, V.; Fiorini, I.; De Filippis, M. P.; Garofalo, A.; Ciani, S. M.; Greco, G.; Novellino, E.; Williams, C. D.; Zisterer, D. M.; Woods, M. J.; Mihai, C.; Manzoni, C.; Mennini, T. Synthesis, Biological Activity, and

SARs of Pyrrolobenzoxazepine Derivatives, a New Class of Specific "Peripheral-Type" Benzodiazepine Receptor Ligands. *J. Med. Chem.* **1996**, *39*, 3435−3450. (c) De Luca, C.; Inesi, A.; Rampazzo, L. *J. Chem. Soc. Perkin Trans. 2* **1985**, 209−212.

(17) Ren, J.; Esnouf, R.; Garman, E.; Somers, D.; Ross, C.; Kirby, I.; Keeling, J.; Darby, G.; Jones, Y.; Stuart, D.; Stammers, D. High-Resolution Structures of HIV−RT from four RT-Inhibitor Complexes. *Nature Struct. Biol.* **1994**, *2*, 293−302.

(18) Ren, J.; Eusnof, R.; Hopkins, A.; Ross, C.; Jones, Y.; Stammers, D. K.; Stuart, D. I. The Structure of HIV-1 Reverse Transcriptase Complexed with 9-Chloro-TIBO: Lessons for Inhibitor Design. *Structure* **1995**, *3*, 915−926.

(19) Hopkins, A. L.; Ren, J.; Esnouf, R. M.; Willcox, B. E.; Jones, E. Y.; Ross, C.; Miyasaka, T.; Walker, R. T.; Tanaka, H.; Stammers, D. K.; Stuart, D. I. Complexes of HIV-1 Reverse Transcriptase with Inhibitors of the HEPT Series Reveal Changes Relevant to the Design of Potent Non-Nucleoside Inhibitors. *J. Med. Chem.* **1996**, *39*, 1589−1600.

(20) Semiempirical quantum-mechanics calculations on benzene and thiophene, using the AM1 and PM3 Hamiltonians available in the MOPAC program (version 6.0, QCPE), indicate that the energy associated with the lowest unoccupied molecular orbital (LUMO) of the latter ring is 0.3 or 0.6 eV, respectively, lower. These data support that the 2-thienyl has a higher propensity with respect to the phenyl substituent to act as electron-acceptor in π-stacking charge-transfer interactions with electron-donor aromatic rings.

(21) Ding, J.; Das, K.; Moereels, H.; Koymans, L.; Andries, K.; Janssen, P. A. J.; Hughes, S. H.; Arnold, E. Structure of HIV-1 RT/TIBO R 86183 Complex Reveals Similarity in the Binding of Diverse Non-Nucleoside Inhibitors. *Nature Struct. Biol.* **1995**, *2*, 407−415.

(22) Mager, P. P. Evidence of a Butterfly-Like Configuration of Structurally Diverse Allosteric Inhibitors of the HIV-1 Reverse Transcriptase. *Drug Des. Discovery* **1996**, *14*, 241−257.

(23) This apparent discrepancy could be due to genetic variability that exists among HIV-1 wild types and laboratory strains such as HIV-1wt and HIV-1III Ba-L. This variability can possibly account for the different antiviral activity shown by the tested compounds with respect to the viral strain used in the assays.

(24) De Clercq, E. Toward Improved Anti-HIV Chemotherapy: Therapeutic Strategies for Intervention with HIV Infections. *J. Med. Chem.* **1995**, *38*, 2491−2517.

(25) High subcutaneous doses of these compounds may be irregularly absorbed in mice, but because of methodological limitations these doses were necessary for quantification in mouse tissue. This enabled us to establish that compounds of this type achieve higher concentrations in the mouse brain than in plasma, although plasma levels were generally below the limit of quantification, precluding any estimate of the brain-to-plasma ratios.

(26) Brain concentrations of **13i** were not corrected for the compound contributed by residual blood because in terms of concentrations this amounted to less than 1% of the brain concentrations.

(27) SYBYL Molecular Modeling System (version 6.2); Tripos Inc., St. Louis, MO.

(28) Bernstein, F. C.; Koetzle, T. F.; Williams, G. J. B.; Meyer, E. F., Jr.; Brice, M. D.; Rodgers, J. R.; Kennard, O.; Shimanouchi, T.; Tasumi, T. The Protein Data Bank: A Computer Based Archival File for Macromolecular Structures. *J. Mol. Biol.* **1977**, *112*, 535−542.

(29) Dewar, M. J.; Zoebisch, E. G.; Healy, E. F.; Stewart, J. J. P. AM1: A New General Purpose Quantum Mechanical Molecular Model. *J. Am. Chem. Soc.* **1985**, *107*, 3902−3909.

(30) Stewart, J. J. P. Optimization of Parameters for Semiempirical Methods. 1. The PM3 Methodol. *J. Comput. Chem.* **1989**, *10*, 209−220.

(31) Maga, G.; Amacker, M.; Ruel, N.; Hubsher, U.; Spadari, S. Resistance to Nevirapine of HIV-1 Reverse Transcriptase Mutants: Loss of Stabilizing Interactions and Thermodynamic or Steric Barriers are Induced by Different Single Amino Acid Substitutions. *J. Mol. Biol.* **1997**, *274*, 738−747.

(32) Weislow, O. W.; Kiser, R.; Fine, B.; Bader, J.; Shoemaker, R.; Boyd, M. R. New Soluble-formazan Assay for HIV-1 Cytopathic Effects: Application of High-flux Screening of Synthetic and Natural Products for AIDS-antiviral Activity. *J. Natl. Cancer Inst.* **1989**, *81*, 577−586.

(33) Perno, C. F.; Yarchoan, R.; Cooney, D. A. Inhibition of Human Immunodeficiency Virus (HIV-1/HTLV−III−Ba-l) Replication in Fresh and Cultured Human Peripheral Blood Monocytes/Macrophages by Azidothymidine and Related 2′,3′-Dideoxynucleosides. *J. Exp. Med.* **1988**, *168*, 1111−1125.

(34) Sodroski, J. G.; Rosen, C. A.; Haseltine, W. A. Trans-acting Transcriptional Activation of the Long Terminal Repeat of Human T Lymphotropic Viruses in Infected Cells. *Science* **1984**, *225*, 381−385.

(35) Popovic, M.; Sarngadharen, M. G.; Read, E.; Gallo, R. C. Detection, Isolation and Continuos Production of Cytopathic Retrovirus (HTLV−III) from Patients with AIDS and pre-AIDS. *Science* **1984**, *224*, 497−500.

(36) Gartner, S.; Markovits, P.; Markovitz, D. M.; Kaplan, M. H.; Gallo, R. C.; Popovic, M. The Role of Mononuclear Phagocytes in HTLV−III/LAV Infection. *Science* **1986**, *233*, 1533−1544.

(37) Karber, G. Beitrag zur Kollektiven Behandlung Pharmakologischer Reihenversuche. *Arch. Exp. Pharmakol.* **1931**, *162*, 480−483.

(38) Bergamini, A.; Perno, C. F.; Capozzi, M. A Tetrazolium-Based Colorimetric Assay for Quantification of HIV-1-Induced Cytopathogenicity in Monocyte-Macrophages Exposed to Macrophage-Colony Stimulating Factor. *J. Virol. Methods* **1992**, *40*, 275−286.

(39) Pauwels, R.; Balzarini, J.; Baba, M. Rapid and Automated Tetrazolium Based Colorimetric Assay for the Detection of Anti-HIV Compounds. *J. Virol. Methods* **1988**, *20*, 309−321.

(40) Chou, T. C. Derivation and Properties of Micaelis-Menten Type and Hill Type Equations for Reference Ligands. *J. Theoret. Biol.* **1976**, *59*, 253−276.

(41) D'Atri, S.; Tentori, L.; Fuggetta, M. P.; Marini, S.; Bonmassar, E. A Miniaturized Cell-mediated Cytotoxicity Assay with Human Effector Mononuclear Cells. *Int. J. Tissue React.* **1986**, *VII* (5), 383−390.

(42) Chou, T. C.; Talalay, I. Quantitative Analysis of Dose−Effect Relationships: the Combined Effects of Multiple Drugs or Enzyme Inhibitors. *Adv. Enzyme Regul.* **1984**, *22*, 27−55.

JM990150O